Structural and electrochemical characterization of yttrium doped barium cerate BaCe0.85Y0.15O3-α for applications in solid oxide fuel cells

G. Raikova, K. Krezhov, I. Genov, Alain Thorel, Anthony Chesnaud, T. Malakova, D. Vladikova, Z. Stoynov

Bulgarian Chemical Communications, Volume 49 Special Issue C (pp. 162 – 170) 2017

Structural and electrochemical characterization of yttrium doped barium cerate $BaCe_{0.85}Y_{0.15}O_{3-\alpha}$ for applications in solid oxide fuel cells

G. Raikova[1]*, K. Krezhov[2], I. Genov[1], A. Thorel[3], A. Chesnaud[3], T. Malakova[2], D. Vladikova[1], Z. Stoynov[1]

[1] *Acad. E. Budevski Institute of Electrochemistry and Energy Systems, Bulgarian Academy of Sciences, 10 Acad. G. Bonchev St., Sofia 1113, Bulgaria*

[2]*Institute for Nuclear Research and Nuclear Energy, Bulgarian Academy of Sciences, 72 bul. Tzarigradsko Shose, Sofia 1784, Bulgaria.*

[3]*Centre des Matériaux, Mines-ParisTech, BP 87, 91003 Evry Cedex, France*

Received January 27, 2017 Revised March 17, 2017

The aim of this work is to achieve a deeper understanding of the conductivity mechanisms in $BaCe_{0.85}Y_{0.15}O_{3-\alpha}$ (BCY15) material displaying good proton conductivity. The study is directly related to the application of BCY15 in an innovative and competitive concept for a high temperature fuel cell operated in reverse mode in the range of 600-700 °C. New approach for combining the information on atomic level by X-ray and neutron-diffraction (ND) and on macro level by impedance spectroscopy for deeper insight into the origin of its mixed (proton and oxide-ion) conductivity is applied. Single-phase $BaCe_{0.85}Y_{0.15}O_{3-\alpha}$ samples with different porosity obtained by addition of graphite powders as pore former and changing sintering conditions were characterized in wet and dry atmosphere and their conductivity was measured in air and hydrogen in wide temperature range. The first neutron diffraction data collected at different temperatures show that the crystal structure of the samples adopts orthorhombic symmetry independently of their porosity and preparation technological conditions. Oxygen vacancies remain random at room temperature. Comparison of the proton and oxide-ion conductivity indicates that at operating temperatures (600-700 ^{o}C) they are equal. The results obtained from the electrochemical studies show that porosity of about 30-35% ensures an optimal microstructure in respect to conductivity and mechanical stability.

Key words: doped perovskite oxides, mixed ionic conductivity, electrochemical impedance spectroscopy, neutron diffraction..

INTRODUCTION

Defect perovskite oxides are intriguing mixed conducting ceramic materials but there are only a few studies on their mixed ionic conducting properties available. The barium cerate based material under study belongs to the extrinsic systems since the defects which enable the charge carriers' transport are activated in the crystal structure by dissolution of water vapour. The proton transport kinetics in the crystal lattice of these materials is closely related to the oxygen vacancies created by the Y substituent. These vacancies can be filled with the oxygen from adsorbed water molecule and the introduced protons will be bound to the lattice oxygen. Thermal activation acts as the driving force for the protons to overcome an energy barrier of a few hundred eV and to jump to another oxygen site, thus constituting proton mobility.

Under humidified hydrogen atmosphere protonic defects are formed by dissociative absorption of water in the presence of oxygen vacancies (Eq.1). It is believed that protons could migrate by hopping from the OH site to oxide ion site at a normal lattice site nearby causing this material to exhibit proton conductivity (Eq. 2) [1-4].

$$H_2O_{(g)} + V_O^{\bullet\bullet} + O_O^x \rightarrow 2OH_O^{\bullet} \quad (1)$$

$$\frac{1}{2}H_{2(g)} + O_O^x \rightarrow OH_O^{\bullet} + e' \quad (2)$$

Water vapour dissociates into a hydroxide ion which fills an oxide-ion vacancy, and a proton that forms a covalent bond with lattice oxygen, i.e. two proton defects are created stoichiometrically [1]. Since the incorporation of water is exothermic [1,4], the protonic transport is dominating at lower temperatures (under 600^{o}C).

The doping with aliovalent rare earth cations brings to the formation of oxygen vacancies and significantly improves the proton conductivity [1-3,5]. In the $BaCeO_3$ system, which is considered to be very promising because of the registered high protonic conductivity (0.01 – 0.05 S/cm between 600-800 ^{o}C [4,5]), the reaction can be described as:

$$2Ce_{Ce}^x + M_2O_3 + O_O^x \rightarrow 2M'_{Ce} + V_O^{\bullet\bullet} + 2CeO_2 \quad (3)$$

To whom all correspondence should be sent:
E-mail: graikova@bas.bg

Proton conductivity in cerates depends on the crystallographic structure, which is a function of temperature and doping concentration. It decreases when transformations to higher symmetry (from orthorhombic to cubic) which bring to equivalent distribution of all oxygen positions and to evenly distributed oxygen ion vacancies take place [1,5]. In addition to the temperature, gas atmosphere and pressure, including water vapor, is detrimental for proton conductivity.

The aim of the present paper is a deeper insight into the conduction mechanism and stability issue for application of BCY15 in a Dual membrane fuel cell (dmFC) which is an innovative SOFC architecture (Fig.1a). Here an oxygen compartment (cathode and oxide ion conducting electrolyte) is combined with a hydrogen compartment (anode and proton conducting electrolyte) through a porous mixed conducting central membrane (CM) where the two types of ions react and produce water which is evacuated through the pores [6-13]. The new design overcomes a principle construction disadvantage connected with the production of water at the electrodes, which brings to dilution of the fuel or oxidizer and reduction of the electrodes catalytic activity.

The key-point of the dmFC development is the design and fabrication of the porous central membrane [10-14]. The first generation Dual Membrane fuel cell was proved by application of a composite central membrane based on the proton conducting $BaCe_{0.85}Y_{0.15}O_{3-\delta}$ (BCY15) and oxide ion conducting $Ce_{0.85}Y_{0.15}O_{1.925}$ (YDC15) electrolyte [10,12,14].

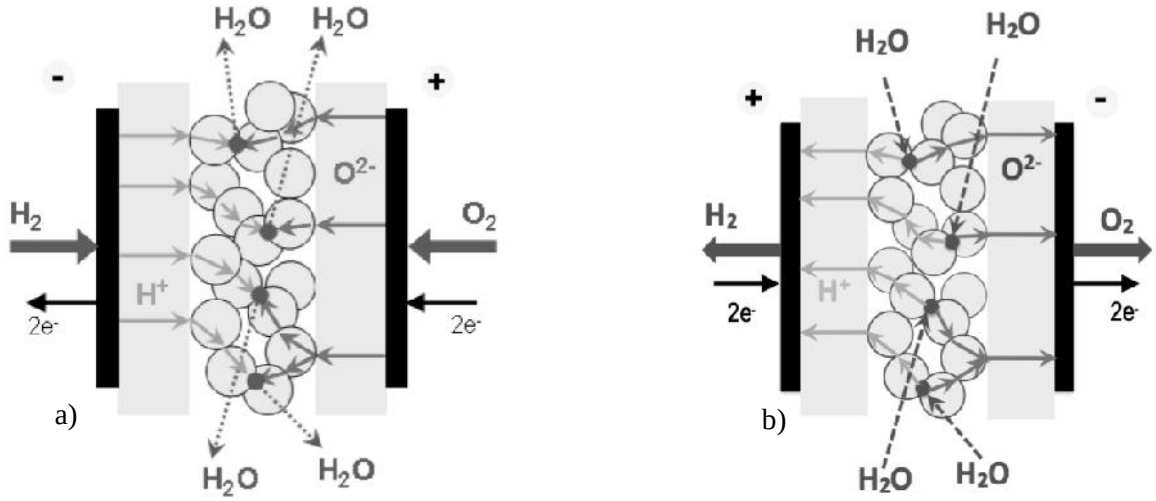

Fig. 1. Schematic representation of the reversible dual membrane fuel cell concept based on a single mixed ion conduction material: a) fuel cell mode of operation; b) electrolyzer mode of operation.

Applying dielectric impedance spectroscopy, a new phenomenon connected with the formation of water as a dipole semi-liquid film in the porous BCY15 structure was discovered. It improves the operation of the dmFC design by decreasing its resistance [11]. In addition, a mixed ionic conductivity in the proton conducting electrolyte BCY15 was registered. Based on the new findings, an innovative trend of dmFC design in which the 3-layered electrolyte assembly (oxide-ion conducting dense electrolyte/porous mixed ion conducting CM/dense proton conducting electrolyte) was fabricated from a single BCY15 material [7]. It is expected that this "monolithic" design will improve the conductivity, the mechanical stability and in consequence the durability of the cell, as well as will simplify the technology. The presence of "water chamber" apriori opens a new opportunity for reversible mode of operation (fuel cell/electrolyzer). The disclosed new phenomena, which define an innovative niche for further improvement of this fuel cell design, need deeper fundamental insight.

The present investigation of the mixed ionic conductivity in the proton conducting electrolyte BCY15 is aimed at obtaining a deeper understanding of the mechanisms which govern this behaviour. Combining the results collected by the techniques based on electrochemical impedance spectroscopy with the advanced methods of the neutron scattering techniques, it is expected to provide reliable information about the transport (diffusion) and hopping in microscopic scale, as well as about the topology of the pores' volume (internal surface areas, porosity, particle size, void size, fractality) at atomic level.

EXPERIMENTAL

The BCY15 powders were fabricated by auto-combustion process starting from metal nitrates and applying urea as reducing agent (Marion Technologies SA, Toulouse, France). Calcination

of the precursor at 1100-1150 ^{o}C in a carrier gas (helium or argon) for complete CO_2 elimination ensured the production of single phase powder with chemical composition $Ba_{1.04}Ce_{0.82}Y_{0.15}O_{3-\alpha}$, determined by ion coupled plasma analysis, with dominating particle size around 200 nm and minor degree of agglomeration.

The BCY15 electrolyte support pellets (diameter/thickness = 20-25/1-1,3mm) were prepared by cold pressing and sintering at heating rate given in Fig. 2. Porous material was obtained by mixing thoroughly the powder BCY15 with graphite powder (2 - 8 wt %) as pore former. The relative porosity (in vol. %) of pellets was evaluated by weighing and measuring the dimensions of the samples which are presented in Table 1. The morphological examinations (Fig. 2) validated that the samples listed in Table 1 have a relatively homogeneous porous structure with a grain size of about 2 microns. Only for sample 1 the average grain size is bigger than 2 microns.

Table 1. Porosity of the samples.

Sample №	1	2	3	4	5	6	7
Porosity, %	9	22	27	35	47	47	48

In order to characterise the changes in the microstructure of the materials, a number of analytical techniques was used: X-Ray Diffraction (XRD) with Energy Dispersive X-ray spectroscopy (EDX), Transmission Electron Microscopy (JEM 200 CX, JEOL Japan) in combination with Electron Dispersive Spectrometry (EDS, TRACTOR, USA) and an ASID 3 D TECNAL 20F ST appliance.

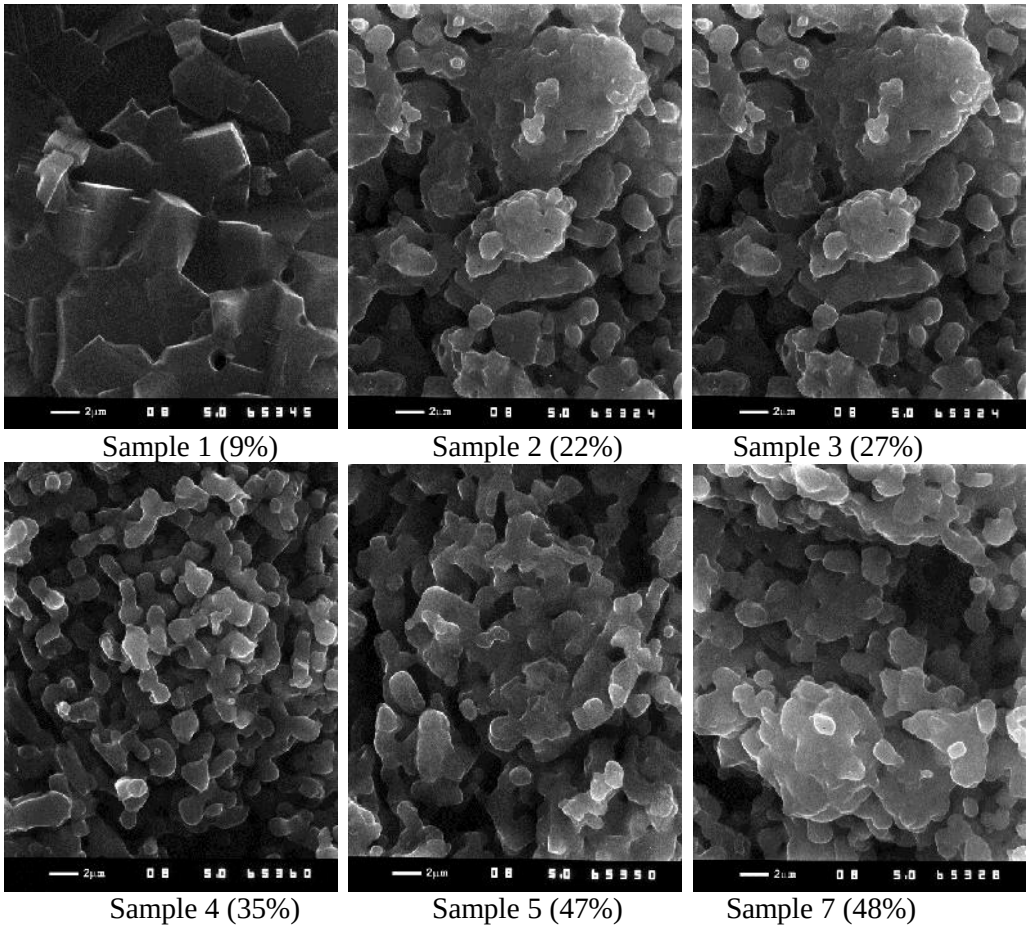

Fig. 2. SEM micrographs of BCY15 samples.

The structural characterization of polycrystalline BCY15 was carried out by X-ray diffraction (XRD) and neuron diffraction (ND). Quantitative phase analyses were done on a Bruker D8 Advanced (filtered Cu radiation; 40kV, 30 mA) diffractometer in Bragg-Brentano geometry. The ND studies were conducted by the time of the flight method (TOF) and the method of constant wavelength (CW). Correspondingly, two instruments were used: the high intensity instrument PSD [15] at the research reactor VVR-M of the Budapest Neutron Centre and the spectrometer DN-12 [16] of JINR, Dubna at the pulsed reactor IBR-2M. The XRD and ND data were analysed using the FULLPROF suite [17] by

applying profile matching mode followed by full profile Rietveld refinement of the structural model. The tabulated coherent scattering lengths b_{coh} were used: 5.07, 4.84, 7.75 and 5.803 fm for Ba, Ce, Y and O, respectively.

The electrochemical characterization of the CM in the monolithic design was conducted by impedance measurements of symmetrical half-cells Pt/BCY15porous/Pt and Pt/BCY15dense/Pt in dry and wet hydrogen and oxygen. Platinum (Metalor) electrodes were painted and sintered in air following a procedure recommended by the producer.

The impedance measurements were performed with IVIUM-CompactStat e10030 in a temperature interval of 100 – 700ºC at frequency range from 1 MHz down to 0,01Hz and density of 5 points/decade. They were done in two modes: potentiostatic and galvanostatic. The half cell measurements were carried out at OCV in working atmosphere wet (3% H_2O) hydrogen.

RESULTS AND DISCUSSION

Some results from the XRD and ND experiments were published previously [18, 19]. Here we supplement the findings with the outcomes from additional experiments aimed to further clarify the structural behaviour of the BCY based materials.

The XRD patterns recorded on samples from fragmented materials after their preparation confirmed that the sintering conditions do not affect in general the single phase structure and the composition of the initial powdered substance BCY15 (Fig. 3). More careful XRD examinations of both sides of BCY15 based pellets showed that the appearance of an additional set of peaks on the upper side of the pellets discloses the presence of a small quantity of $Y_{0.1}Ce_{0.9}O_{2.95}$ (Fig. 3c). This can be due to loss of BaO on the upper surface because of evaporation during the sintering step.

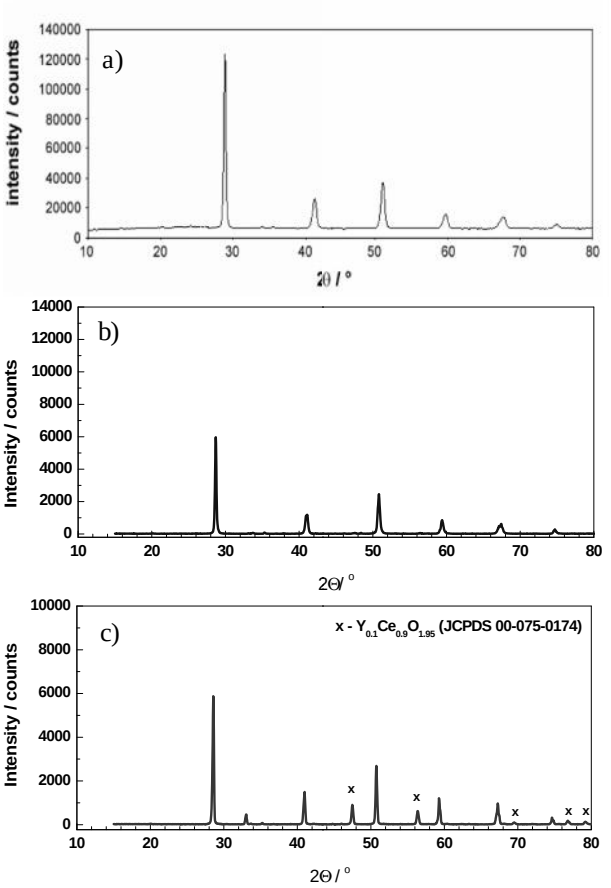

Fig. 3. X-ray diffraction patterns of BCY15: powders according to the producer (a); milled material after cold pressing and sintering (b) and pellets' surface (c).

Fig. 4 shows the neutron diffraction (ND) patterns collected on representative powder samples of the three types of BCY15 based material. There are no any indications of difference in crystallographic symmetry of the particular samples.

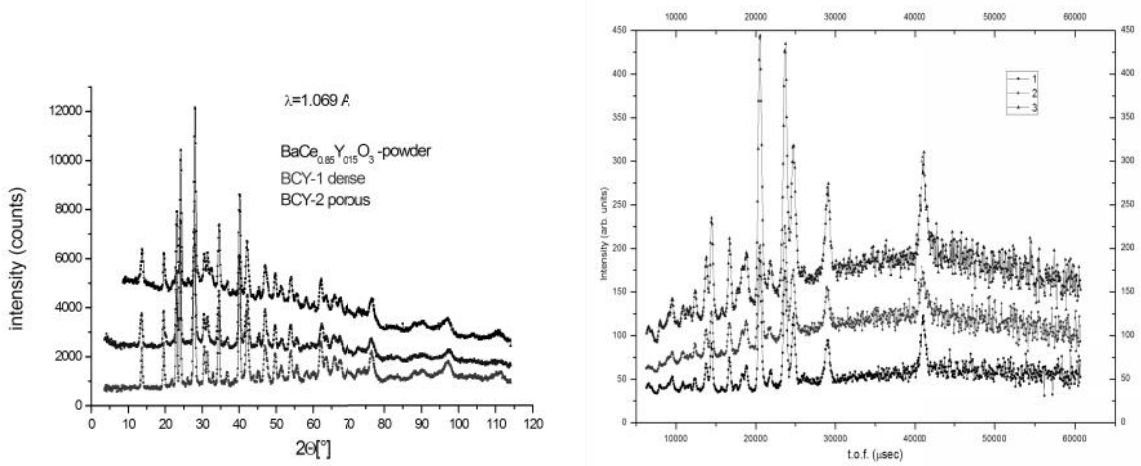

Fig. 4. ND patterns of $BaCe_{0.85}Y_{0.15}O_{3-\delta}$ based samples at 295 K: a) constant wavelength (λ = 1.069 Å) pattern. The sample denoted as powder was kept for three days in moist air; b) TOF patterns: 1 (dense), 2 (porous), 3 (powder). The patterns are vertically shifted to improve visibility.

The patterns could be indexed in rhombohedral space group R-3c and monoclinic symmetry space group I2/m. We have also checked for a mixture of two perovskite phases of R-3c and I2/m symmetry as recommended for compositions with this and higher substitution rates [20-23]. However, in all the cases the structure refinements did not produce better agreement factors than in orthorhombic Pnma.

The multi-pattern mode of the FullProf program for simultaneous treatment of neutron (constant wavelength) and x-ray data sets were used to refine the structure and to determine the lattice parameters, atomic positions and thermal factors. We considered the crystal structure of undoped $BaCeO_3$ as the starting structural model, with orthorhombic symmetry and space group Pnma; all the Bragg peaks of the diagram could be thus indexed. Because the structure contains two different B-site cations the possibility of ordered and disordered variants was checked. Best refinements were produced by models where Yttrium atoms were introduced at random at 4b positions together with Cerium, and the complementary occupancy factors were refined, constrained to a full occupancy. The formula checked was $BaCe_{1-x}Y_xO_{3-0.5x}$, where x=0.15. In the final refinement, the Ce/Y occupancy factors were unconstrained, indicating a slight deviation from the nominal 0.85:0.15 stoichiometry.

Fig. 5 shows on the example of a powdered "dense" material the agreement between the observed and calculated NPD curves in the final multi pattern Rietveld fit. The structure parameters and the discrepancy factors describing the Rietveld fit quality are presented in Table 2.

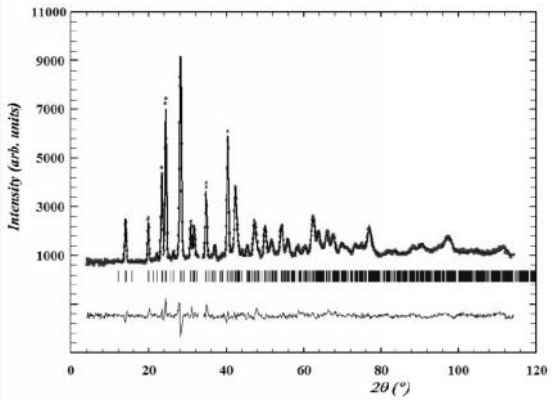

Fig. 5. Observed (crosses), calculated (continuous line), and difference (bottom) Rietveld ND profiles of milled material of dense BCY15 pellet at 295 K. The row of tick marks gives the positions of the allowed Bragg reflections.

The unit cell parameters of $BaCe_{0.85}Y_{0.15}O_{3-\delta}$ are close to the values of $BaCe_{0.9}Y_{0.1}O_{2.95}$ given in the references included in the ICDD PDF-4 database. The relationship between the lattice parameters is typical for O-type perovskites, where the tilting of the oxygen octahedra is the main reason for the deviation from the ideal perovskite structure ABX_3 [24, 25].

Table 2. Refined structural parameters of $BaCe_{0.85}Y_{0.15}O_{3-\delta}$ in space group Pnma. Unit cell parameters (Å): a=6.2089(9), b=8.8292 (6), c=6.2066(8), volume (Å^3) = 340.24(25). Agreement factors (%): R_{wp} =5.92, R_B = 3.66, $\chi 2$= 1.85. Estimated standard deviations are in parenthesis.

	x	y	z	B, Å²
Ba	0.0098(5)	0.25	-0.0028(7)	1.14(5)
Ce	0	0	0.5	0.56(6)
Y	0	0	0.5	0.56(6)
O1	0.5212(5)	0.25	-0.0792(7)	0.86(6)
O2	0.2674(4)	0.0395(7)	0.7249(7)	0.86(6)

Fig. 6 illustrates the agreement between the observed and calculated ND curves after the Rietveld refinement. Table 3 presents the structure parameters of a BCY15 pellet (Left panel).

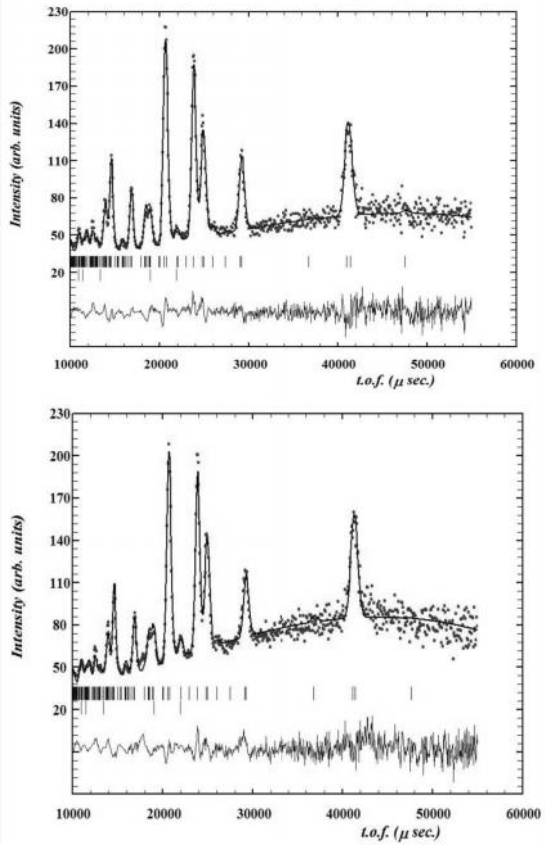

Fig. 6. Observed (crosses), calculated (continuous line), and difference (bottom) Rietveld ND profiles at 295 K. Left: BCY15 based pellet; Right: as received BCY15 powder without temperature treatment. The row of tick marks gives the positions of the allowed Bragg reflections.

The pelletized BCY15 material without pore former (graphite) was sintered at 1400 ^{o}C for 8 hours in air. The TOF diffraction data were taken for 6 hours at 295 K. The prolonged sintering resulted into a more compact unit cell. Right panel gives the diffraction pattern of BCY15 powder before the usual temperature annealing at 1000^{o}C aiming to reduce possible consequences of sample transportation to JINR. In both panels the lines originating from the aluminium foil of the sample holder are distinctly observable. The quantitative phase analysis yields below 1.2% Al for the second phase.

Here is to recall that the ideal perovskite structure is cubic (Pm–3m) in which the B-cations are surrounded by six anions arranged in corner-sharing octahedral geometry. This arrangement forms cubooctahedral cavity in which the A-cation is placed. Many functional properties observed in perovskite oxides ABO_3 exhibit close couplings to slight structural distortions in the perovskite lattice that consist of this three-dimensional network of corner-sharing BO_6 octahedra. In general the distortion of the ideal perovskite structure of oxides is manifested by (1) cooperative tilting (in-phase and/or antiphase rotations) of the BO_6 octahedra; (2) deformation of the BO_6 octahedra and (3) displacement of the B-cation from the center of the octahedra. The documentation of such distortions and elucidation of their influence on properties have been important issues in fundamental materials science investigations, as well as for the broad range of applications of oxide materials.

Fig.7 and Fig.8 illustrate on the example of a BCY15 pellet of 13% porosity the attempt to understand the structural accommodation to working temperature.

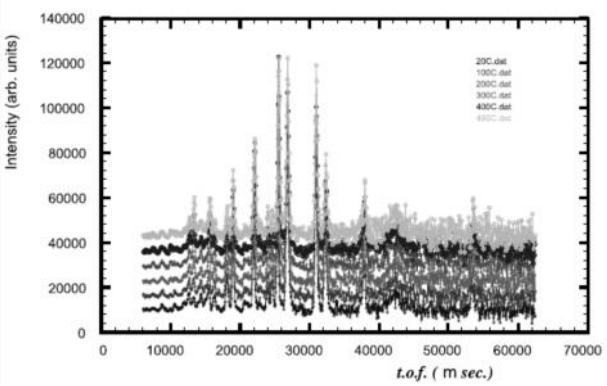

Fig. 7. Successive TOF patterns taken at stabilized temperatures in increasing order (in ^{o}C): 20, 100, 200,300, 400, 480. The patterns are vertically shifted to improve visibility.

The careful examination of the Rietveld fits to the set of temperature dependent diffraction patterns (at 480 ^{o}C is the one presented) showed that although the unit cell volume is steadily expanding with increasing temperature (see Fig.9) the counting statistics of present experiment was not sufficient to provide outside the error limits sound grounds in deriving irrefutable conclusions regarding the subtle structural changes. Nevertheless the trends in structure development validate that in the investigated materials based on $BaCe_{0.85}Y_{0.15}O_{3-\delta}$ the tilting of the $(Y\text{-}Ce)O_6$ octahedra is reasoning the orthorhombic symmetry observed.

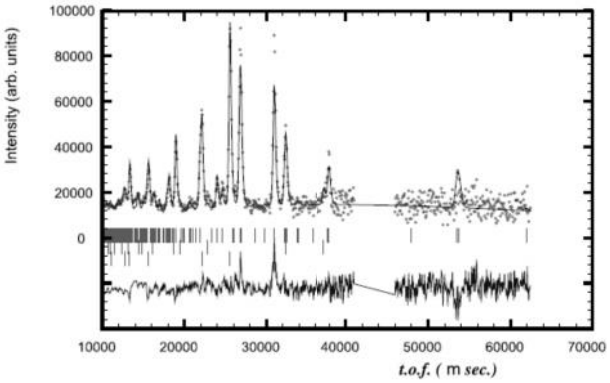

Fig. 8. Observed (crosses), calculated (continuous line), and difference (bottom) Rietveld ND profiles at 480 ^{o}C. The rows of tick marks give the positions of the allowed in Pnma space group Bragg reflections for the main phase of BCY15 (upper) and the minor contribution of Al foil (middle) and Cu heater (lower). The affected region of the pattern because of experimental geometry is excluded from the refinement.

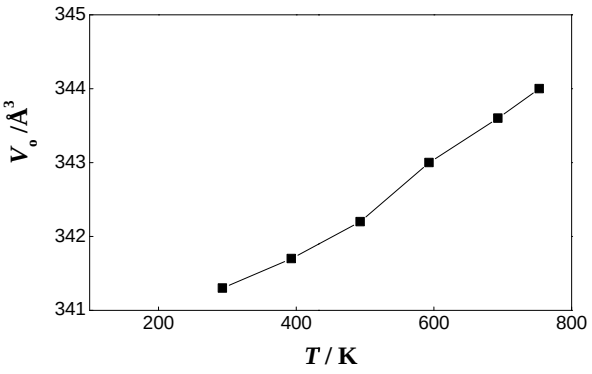

Fig. 9. Temperature dependence of unit cell volumeV_o of BCY15 pellet of 13% porosity.

On the other hand, Fig.10 illustrates the attempt to understand the impact of water on the BCY15 structure. In this experiment several drops of water with consecutive stirring were applied to achieve homogeneous humidification of the powder before carrying out the measurement of the so-protonated sample.

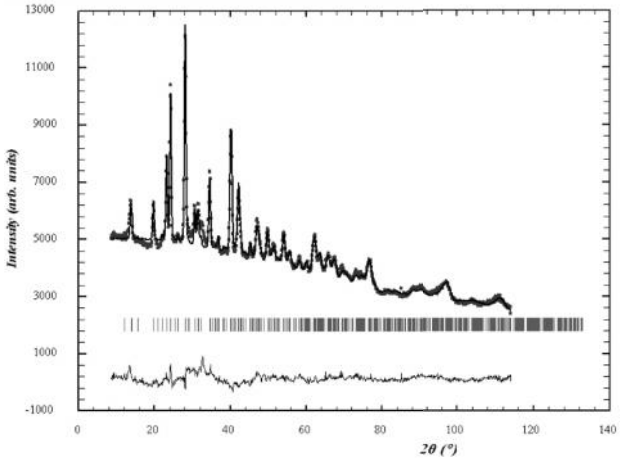

Fig. 10. Observed (crosses), calculated (continuous line), and difference (bottom) NPD Rietveld profiles of BCY15 protonated powder at 295 K. The row of tick marks gives the positions of the allowed Bragg reflections.

The extensive incoherent scattering of hydrogen from the hydroxyl groups is reflected by the steadily rising contribution to the background with decreasing to zero scattering angles. The fit is not of the required quality to allow for drawing up unambiguous conclusions for the structural details. By simultaneous treatment of multiple powder diffraction datasets obtained by present constant wavelength X-ray and neutron diffraction experiment the powder overlap problem is partially resolved in a Rietveld refinement. The effect of the multi pattern Rietveld analysis is effectively the deconvolution of overlapping reflections by differing shifts in their relative positions. The medium resolution neutron powder data however have restricted the solution of the peak overlap problem in the structure models with protons.

In summary, the neutron diffraction experiments performed so far have shown that the BCY15 based materials are anion deficient perovskites. The crystal structure of these materials adopts orthorhombic symmetry independently of the technological preparation of the samples (sintering conditions, presence of pore former etc.) and microstructure, including porosity. In their structures oxygen vacancies remain random at room temperature. The actual long range atomic order strongly reflects the storage conditions, annealing temperature and humidity.

In addition to the deeper structural characterization, the investigated BCY micro-samples which present components (electrolyte and central membrane) of the dual membrane cell were investigated in respect to their conductivity in both air and hydrogen, which gives the possibility to register mixed ion conductivity and to compare it.

Characteristic impedance diagrams for one and the same sample measured in the two selected atmospheres are presented in Fig. 11.

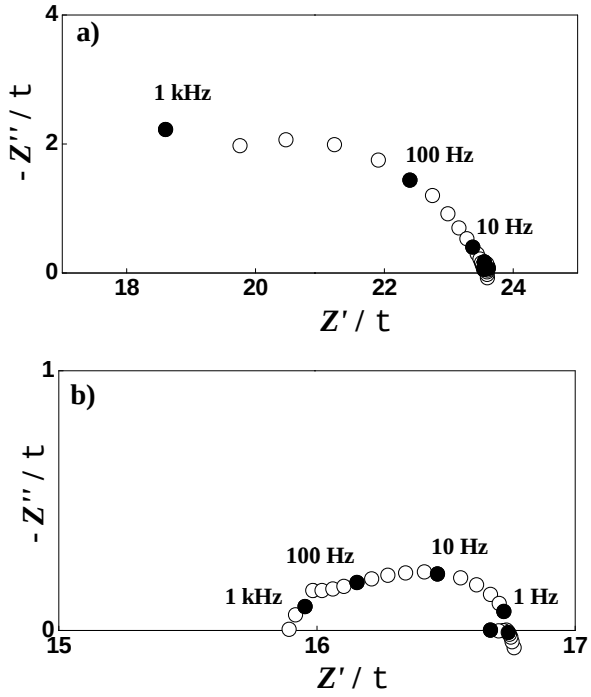

Fig. 11. Complex plane impedance diagrams of sample 3 (27% porosity) measured in dry air (a) and wet hydrogen (b) at 700°C.

The resistance values obtained from the impedance measurements at different temperatures were used for the construction of the Arrhenius plots (Figs. 12, 13):

$$\rho = A/T \exp(-E_a / kT) \qquad (4)$$

where ρ is the resistivity, A is the pre-exponential term, k is the Boltzmann constant, E_a is the activation energy and T is the temperature in K.

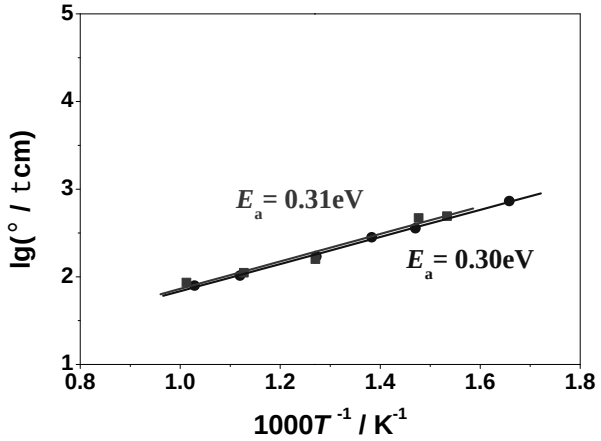

Fig. 12. Arrhenius plots of sample 4 (35% porosity) measured in dry air (●) and wet hydrogen (■).

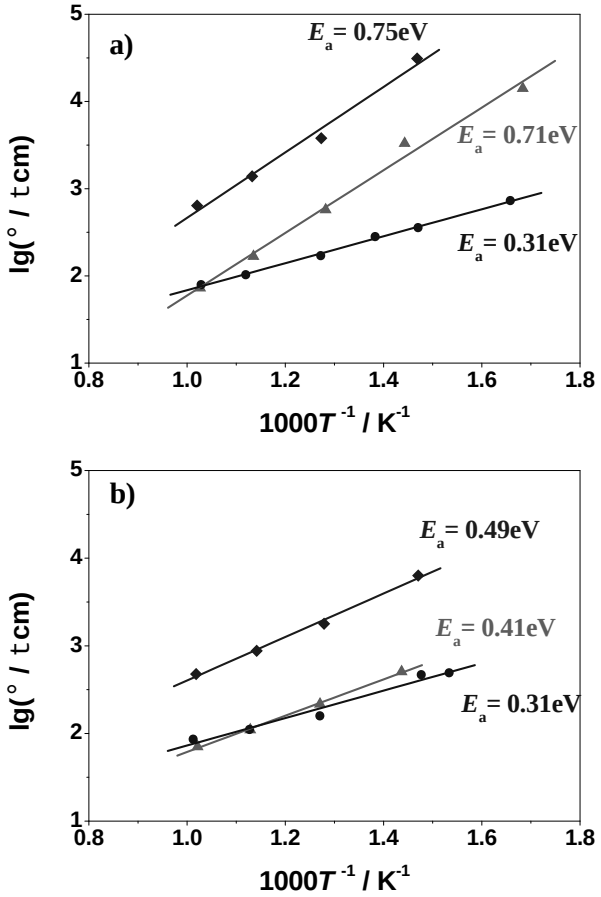

Fig. 13. Arrhenius plots of BCY15 samples with different porosity measured in dry air (a) and wet hydrogen (b): (◆) - sample 5 (47% porosity), (▲) - sample 4 (35% porosity), (●) - sample 3 (27% porosity).

The results show that oxide ion conductivity is more sensitive to samples microstructure (25-35% porosity) at low temperatures, whereas at operating temperatures the effect of porosity decreases, while proton conductivity is less sensitive to porosity in the whole temperature range. At operating temperatures 650-700 ^{o}C the proton and oxide ion conductivities of BCY15 electrolyte are equal. It is interesting to note that the change of the porosity in the limits 25-35% does not influence the mixed conductivity. This result is important for the optimization of the CM which has to combine high conductivity with sufficient porosity.

CONCLUSIONS

Mixed proton and oxide-ion conductivity of ceramic BCY15 is an attractive property for its application as an electrolyte in a new design of a fuel cell which eliminates the formation/evacuation of the water produced during operation from the electrodes. New approach for combining the information on atomic level by ND and on macro level by impedance for deeper insight into the conductivity mechanisms is applied. It needs further development. The results obtained from the combined electrochemical and structural studies of BCY15 in addition to its natural property to split water reinforce a new emerging niche for development of other materials with similar structure and mixed conductivity which will further stimulate the development of the dual membrane fuel cell concept for operation in both fuel cell and electrolyzer mode.

Acknowledgements: *The research leading to these results has received funding from Bulgarian NSF under grant No E02/3/2014. The authors express their gratitude to Prof. E.Svab and Dr. M. Fabian from the Budapest Neutron Centre and Prof. D. Kozenko and his team (Dr. S. Kichanov and Dr. E. Lukin) from the FLNP laboratory of JINR - Dubna for constructive discussions and help in execution of neutron beam experiments.*

REFERENCES

1. L. Malavasi, C. Fisher, M. Islam, *Chem. Soc. Rev*., **39**, 4370 (2010).
2. T. Ishihara, N. Sammes, O. Yamamoto in High Temperature Solid Oxide Fuel Cells: Fundamentals, Design and Applications, edited by S.C. Singhal and K. Kendall, (Elsevier, 2003) pp. 83-117.
3. H. Iwahara, *Solid State Ionics*, **86-88**, 9 (1996).
4. A. Bassano, V. Buscaglia, M. Viviani, M. Bassoli, M-T. Buscaglia, M. Sennour, A. Thorel, Nanni, *Solid State Ionics*, **180**, 168 (2009).
5. N. Bonanos, K. Knight, B. Ellis, *Solid State Ionics*, **79**, 161 (1955).
6. Patent N^{o}0550696000 March l7th, 2005 "Cellule de Pile a Combustible Haute Temperature a Conduction Mixte Anionique et Protonique" extended internationally in 2007, invented by the Centre des Materiaux d'Evry, common research center to ARMINES and MINES ParisTech.
7. A. Thorel, Z. Stoynov, D. Vladikova, A, Chesnaud, M. Viviani, S. Presto," Fuel Cell with Monolithic Electrolytes Membrane Assembly", Parent N^{o} 20120156573, 21.06.2012.
8. A. S. Thorel, A. Chesnaud, M. Viviani, A. Barbucci, S. Presto, P. Piccardo, Z.llhan, D. Vladikova, Z. Stoynov, "IDEAL-CeII, a high tempersture Innovative Dual mEmbrAne fueL-Cel/" in: Solid Oxide Fuel Cells (SOFC XI), The Electrochemical Society Proceedings Series, Pennington, NJ (2009) 753.
9. D. Vladikova. Z. Stoynov, G. Raikova, A. Thorel, A. Chesnaud, J. Abreu, M. Viviani, A. Barbucci, S. Presto, P. Carpanese "Impedance Spectroscopy Studies af Dual Membrane Fuel Cell", *Electrochimica Acta*, **56,** 7955 (2011).
10. M. Viviani, S. Presto, A. Barbucci, M. Carpanese, R. Amendol, A.Thorel, A. Chesnaud, J. Abreu, R. Costa, Z.llhan, S. Ansar, D. Vladikova, Z. Stoynov, "Proton and Mixed Conductors for Dual Membrane Fuel

Cells", MRS Proceedings, 2011, Vol. 1330, mrss11l-1330-j05-04.
11. Z. Stoynov, D Vladikova, E. Mladenova, *Journal of Solid State Electrochemistry*, **17,** 555 (2013), DOI 10.1007/s10008-012-1916-z.
12. Massimo Viviani, Alain Thorel, Antonio Barbucci, Daria Vladikova, Anthony Chesnaud, Ivaylo Genov, Gergana Raikova, Elisa Mercadelli, Paolo Piccardo, Maria Paola Carpanese, Zdravko Stoynov, Sabrina Presto, and Alessandra Sanson, *ECS Trans.,* **57(1)**, 3143 (2013)
13. D. Vladikova, Z. Stoynov, A. Chesnaud, A. Thorel, M. Vivianu, A. Barbucci, G. Raikova, P. Carpanese, M. Krapchanska, E. Mladenova, *International Journal of Hydrogen Energy*, **39(36)**, 21561 (2014).
14. K. Przybylski, J. Prazuch, T. Brylewski, R. Amendola, S. Presto and M. Viviani, in Proc. Intern. Workshop Advances and Innovations in SOFCs, edited by D. Vladikova and Z. Stoynov (IEES, Sofia, 2011), pp. 62 -71.
15. Web site of Budapest Neutron Centre. Retrieved from: http://www.bnc.hu
16. Web site of IBR2 User Club. Retrieved from: http://ibr-2.jinr.ru.
17. J. Rodriguez-Carvajal, *Physica B*, **192**, 55 (1993); FullPrf Suit, a set of crystallographic programs. Retrieved from:https://www.ill.eu/sites/fullprof
18. K. Krezhov, D. Vladikova, G. Raikova, I. Genov, T. Malakova, D. Dimitrov, E. Svab, M. Fabian, "Structure study of BaCe0.85Y0.15O3-Δ as solid state fuel cell material", AIP Conf. Proc. vol.1722, 140008 (2016); http://doi.org/10.1063/1.4944198.
19. K. Krezhov, D. Vladikova, G. Raikova, T. Malakova, I. Genov, Tz. Nonova, E. Svab, M. Fabian, "$BaCe_{0.85}Y_{0.15}O_{3-\Delta}$ Based Materials for Solid Oxide Fuel Cells: Room Temperature Neutron Diffraction Study", RAD Proceedings, vol.1, issue 1 pp.117-123, Apr. 2016, DOI: 10.21175/RadProc.2016.28
20. K. Takeuchi, C. K. Loong, J. W. Richardson, Jr. J. Guan, S. E. Dorris and U. Balachandran, *J. Sol. St. Ionics*, **138**, 63 (2000).
21. K. S. Knight, "Oxygen Vacancy Ordering in NeodymiumDoped Barium Cerate," Sol. St. Comm., vol. 112, no. 2, pp. 73-78, Sep. 1999.
22. C.K. Loong, M. Ozawa, K. Takeuchi, U. Koichi and N. Koura, "Neutron Studies of Rare Earth-Modified Zirconia Catalyst and Yttrium-Doped Barium Cerate Proton-Conducting Ceramic Membranes," J. Alloys Compd., vol. 408-412, pp. 1065–1070, Feb. 2006.
23. D. Han, M. Majima and T. Uda, "Structure Analysis of 18. $BaCe_{0.8}Y0.2O_{3-\delta}$ in Dry and Wet Atmospheres by HighTemperature X-Ray Diffraction Measurement," J. Sol. St. Chem., vol. 205, pp. 122–128, Sep. 2013.
24. A. Glazer, "The classification of tilted octahedral in perovskites", *Acta Cryst*., **B28**, 3384 (1972).
25. A. Glazer, "Simple ways of determining perovskite structures", *Acta Cryst*., **A31**, 756 (1975)

СТРУКТУРНО И ЕЛЕКТРОХИМИЧНО ОХАРАКТЕРИЗИРАНЕ НА ИТРИЕВО ДОТИРАН БАРИЕВ ЦЕРАТ $BaCe_{0.85}Y_{0.15}O_{3-\alpha}$ ЗА ПРИЛОЖЕНИЕ В ТВЪРДООКСИДНИ ГОРИВНИ КЛЕТКИ

Г. Райкова[1*], К. Крежов[2], И. Генов[1], А. Торел[3], А. Чесно[3], Т. Малакова[2], Д. Владикова[1], З. Стойнов[1]

[1] Институт по електрохимия и енергийни системи „Акад. Евгени Будевски", Българска академия на науките, ул. Акад. Г. Бончев, бл.10, София 1113, България
[2] Институт за ядрени изследвания и ядрена енергетика, Българска академия на науките, бул. „Цариградско шосе" 72, София 1784, България.
[3] Център по материалознание, Париж, BP 87, 91003 Иври Седекс, Франция

Постъпила на 27 януари 2017 г.; коригирана на 17 март 2017 г.

(Резюме)

Цел на настоящата работа е задълбочено изучаване механизмите на проводимост на материали от типа $BaCe_{0.85}Y_{0.15}O_{2.925}$ (BCY15), които са известни с добрата си протонна проводимост. Изследването е пряко свързано с приложението на BCY15 в иновативна концепция за високотемпературна горивна клетка, работеща в обратим режим при 600-700° C. За по - дълбоко вникване в причините обуславящи смесената проводимост (протони и кислородни йони) на този материал е приложен нов подход, които комбинира информацията получена от рентгенова- и неутронна дифракция (НД) на атомно ниво с тази получена от прилагане на импедансна спектроскопия на макро ниво Еднофазни BaCe0.85Y0.15O3- α образци с различна порестост, получена чрез добавяне на порообразувател графит на прах и чрез различни условия на синтероване са охарактеризирани във влажна и суха атмосфери. Измерена е тяхната проводимост във въздух и във водород в широк температурен диапазон. Първите данни, получени от неутронно- дифракционни изследвания при различни температури показват, че кристалната структура, която притежава орторомбична симетрия, не зависи от порестостта и условията на синтероване. Кислородните ваканции в структурата остават произволно разпределени при стайна температура. Сравнението на протонната и кислородната проводимост показва, че при работни температури (600-700 °C) те са равни. Резултатите от електрохимичните изследвания показват, че 30-35% пористост е оптималната микроструктура по отношение на проводимост и механична стабилност.